Role of the substrate strain in the sheet resistance stability of NiSi deposited on Si(100)

Cite as: Journal of Applied Physics **85**, 3614 (1999); https://doi.org/10.1063/1.369774
Submitted: 24 August 1998 • Accepted: 05 January 1999 • Published Online: 22 March 1999

Eliane Maillard-Schaller, B. I. Boyanov, S. English, et al.

Role of the substrate strain in the sheet resistance stability of NiSi deposited on Si(100)

Eliane Maillard-Schaller,[a] B. I. Boyanov, S. English, and R. J. Nemanich
Department of Physics, North Carolina State University, Raleigh, North Carolina 27695-8202

(Received 24 August 1998; accepted for publication 5 January 1999)

In order to study the influence of strain on the formation and stability of NiSi, Ni has been deposited on strained and relaxed Si(100) *n*-type substrates. Strained Si substrates have been produced by depositing a pseudomorphic silicon film onto a 3000 Å thick relaxed $Si_{0.8}Ge_{0.2}$ film. Raman spectroscopy has established that the silicon film is strained. The presence of a characteristic cross-hatch pattern has been identified by atomic force microscopy. Measurements show that the sheet resistance (R_s) of the silicide formed on strained silicon remains stable up to 700 °C while the R_s of the silicide formed on bulk silicon (100) shows a significant increase at 600 °C. X-ray photoelectron spectroscopy shows that the NiSi–$NiSi_2$ phase transition occurs at a higher temperature and is, therefore, not responsible for the R_s instability. Scanning electron microscopy measurements indicate that islanding occurs in the temperature region of the resistivity increase. Photoelectron emission microscopy has been employed to observe the surface morphology during annealing, and islanding is not observed until a higher annealing temperature for the NiSi on strained Si. The increase in R_s is apparently correlated to the islanding of NiSi which appears at lower temperature on the bulk silicon substrate than on the strained silicon substrate. The stability of the NiSi film on the strained Si substrate is related to the strain induced by thermal expansion and the increased lattice constant of the strained Si. © *1999 American Institute of Physics.* [S0021-9606(99)05107-7]

I. INTRODUCTION

Silicides used in very large scale integrated circuits as contact materials to the source and drain areas must show a metal-like conductivity while sustaining the high temperature thermal treatment used in manufacturing. Nickel monosilicide (NiSi) is one of the most promising candidates for the next generation of deep submicron integrated circuits. The formation of Ni silicides on Si has been extensively studied.[1–3] It has been shown that the interface reaction initiates with Ni_2Si formation at ~200 °C followed by NiSi formation at ~500 °C and finally by $NiSi_2$ formation at ~800 °C. The $NiSi_2$ phase is the final phase, and it grows epitaxially on Si(100), (110), and (111).[4] As the sheet resistivity of the silicide is increasing from 20 to 50 $\mu\Omega$ cm with the transition from NiSi to $NiSi_2$, the thermal stability of the NiSi is of primary importance for technical applications.

The thermal stability of NiSi depends on the phase transition from NiSi to $NiSi_2$ and on the morphology stability of the NiSi film. The phase transition to $NiSi_2$ is controlled by nucleation phenomena which occur at a temperature of ~300 °C above the conditions required for the diffusion controlled growth of NiSi.[3] The interface between the silicide and the substrate is therefore very important. Steps at the interface apparently delay the formation of the epitaxial $NiSi_2$ by the presence of a higher kinetic reaction barrier at the growth front.[5] On the other hand, if the nucleation density is limited as is the case for narrow lines in integrated circuit applications, then complete conversion is not ensured,[6] and the formation of $NiSi_2$ is delayed. In the literature, the phase transition is characterized by x-ray photoelectron spectroscopy (XPS),[7,8] ultraviolet photoelectron spectroscopy,[9] Rutherford back scattering,[8] or x-ray diffraction.[10]

The stability of the sheet resistance, R_s, of the silicide depends on its morphology too, since the conductivity of a defective silicide film or a system of islands is lower than the conductivity of a defect-free, continuous silicide film.[11] The morphology is usually characterized by scanning electron microscopy (SEM),[12] atomic force microscopy (AFM),[13] and transmission electron microscopy,[6,14] and seems to be mainly influenced by the interface energy.[15]

In this article, the influence of the Si substrate strain on the thermal stability of the NiSi will be presented. The approach that will be employed is to prepare pseudomorphic strained Si layers through molecular beam epitaxy (MBE) growth on relaxed $Si_{1-x}Ge_x$ layers.[16] The reacting Ni layer is deposited *in situ* so the interface is atomically clean, and the reaction is not limited by contaminants.

Pseudomorphic strained Si films have been chosen in order to isolate the effect of strain on the NiSi stability. In itself, strained Si films are also attracting a considerable interest. The biaxial strain in the Si film causes a splitting of the conduction band degeneracy. This then results in a higher electron mobility and an improvement of the performance of existing semiconductor technology without major changes in the process flow.[17,18]

Since $Si_{1-x}Ge_x$ alloys have a larger lattice constant than Si, a Si film deposited on a relaxed $Si_{1-x}Ge_x$ alloy film will be in biaxial tension, and the Si unit cell will deform from its

[a]Present address: Physics Department, University of Fribourg, 1700 Fribourg, Switzerland; electronic mail: eliane.schaller@unifr.ch

bulk cubic state. If the Si film thickness is increased, the strain energy will be large enough to cause the formation of an array of interface misfit dislocations which results in relaxation of the Si epitaxial layer towards the bulk Si value. If the thickness of the Si layer is below a critical value, the in-plane lattice constant of the layer will match that of the substrate.[18] The lattice constant of $Si_{1-x}Ge_x$ increases with Ge content, therefore as the Ge content increases, the strain in the epitaxial Si layer will also increase.[17] The critical thickness of the Si layer is, as a result, reduced. In this study, $Si_{0.8}Ge_{0.2}$ has been used as substrate. According to equilibrium theory the critical thickness for a Si layer will be ~150 Å.[19,20] However, results have established that low temperature growth can result in a metastable Si film which can sustain the strain at thicknesses greater than the equilibrium thickness. For the 550 °C growth temperature employed in this study, the Si layer will be metastable for critical thicknesses up to 1000 Å.

Raman scattering is employed to determine the strain in the epitaxial Si layer. Variations of the silicide R_s are correlated to SEM and XPS measurements. Moreover, photoelectron emission microscopy (PEEM) is employed for *in situ* observation of the changes of the surface morphology during annealing.

II. EXPERIMENT

Thin films of Ni (100 Å thick) have been deposited on *n*-type Si(100) and strained silicon substrates by ultrahigh vacuum (UHV) electron beam evaporation. The strained silicon substrates have been produced by deposition of a pseudomorphic silicon film (400 Å) on top of a 3000-Å-thick relaxed $Si_{0.8}Ge_{0.2}$ film. The $Si_{0.8}Ge_{0.2}$ film was prepared by MBE at 550 °C in a dual e-gun system with a base pressure of 2×10^{-10} Torr. The resistivity of the silicon substrate was 0.8–1.2 Ω cm, and the $Si_{0.8}Ge_{0.2}$ and Si pseudosubstrates were not intentionally doped. Before deposition, atomically clean Si surfaces were prepared by spin etching the Si(100) substrates with a 1:1:10 HF:H_2O:ethanol solution, followed by *in situ* thermal desorption at 900 °C and deposition of a 200-Å-thick homoepitaxial Si buffer layer at 550 °C. Deposition of the $Si_{0.8}Ge_{0.2}$ and the Si films was controlled with quartz crystal thickness monitors. The deposition rates were below 0.5 Å/s. After thermal cleaning and after deposition, low energy electron diffraction (LEED) displays a (2×1) reconstruction pattern and XPS confirms the absence of any oxygen contamination at the surface.

Subsequent to Ni deposition, the samples were annealed *in situ* for 20 min at temperatures ranging from 300 to 1000 °C. XPS measurements have been performed *in situ* in a VG Clam II spectrometer.

The two deposition chambers, the XPS system, the LEED system, and the Auger system are all components of an integrated processing system with an UHV sample transfer chamber that allows preparation and characterization of surfaces and films.

Sheet resistance measurements using a linear four-point probe have been performed *ex situ* after sample cooling. AFM measurements have been performed with the sample in air using a M5 Park Scientific scanning tunneling microscope AFM. Raman spectroscopy has been performed with an ISA Jobin Yvon U1000. The Raman spectra were excited with 514.5 nm light from an Ar ion laser. SEM images of the NiSi films have been obtained in a JEOL JSM-6400F.

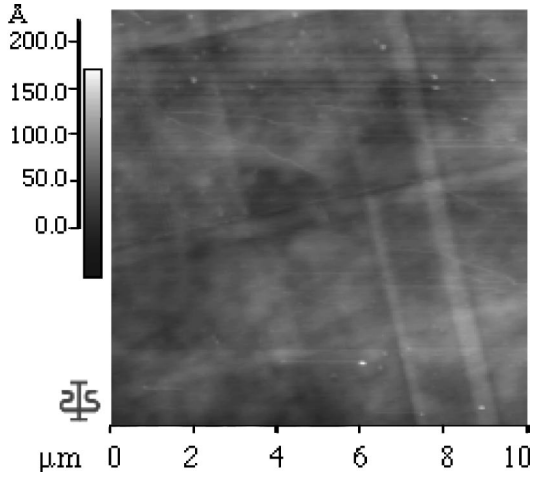

FIG. 1. AFM image of the strained silicon surface showing the characteristic ⟨110⟩ cross-hatch pattern. The dislocation lines are ~25 nm wide at a separation distance of 1–4 μm.

PEEM has been performed in a custom PEEM system from Elmitech Corp. In this system, the sample is illuminated by a 100 W Hg lamp which exhibits a high energy cutoff at 5.1 eV. The sample is at −20 kV relative to an anode 2 mm in front of the surface. An image is formed by photoelectrons emission from the surface. Contrast from different regions on the sample surface will depend on the photothreshold of the exposed surface material.[21,22]

III. RESULTS AND DISCUSSION

Strained Si substrates have been produced by deposition of Si on top of a 3000 Å thick relaxed $Si_{0.8}Ge_{0.2}$ film. The relaxed Si_xGe_{1-x} alloy films grown on Si(100) show a ⟨110⟩ cross-hatch pattern of dislocation lines.[23] Figure 1 shows an AFM scan of the substrate surface after the Si deposition. The Si film presents the same morphology as the $Si_{0.8}Ge_{0.2}$ substrate indicating that the relaxation of the lattice is maintained. As the lattice parameter of $Si_{0.8}Ge_{0.2}$ (5.47 Å) is 0.7% larger than the lattice parameter of Si (5.43 Å), the Si layer is under tensile stress.

Raman spectroscopy has been performed on the epitaxial structure in order to determine the tensile strain of the pseudomorphic Si layer. The Si peak around 520 cm^{-1} is displayed in Fig. 2. Fits of the Raman peak show the main Si–Si vibration at 520 cm^{-1} due to the bulk Si substrate, a component at 513 cm^{-1} attributed to the Si–Si vibration in the tensile-strained Si layer, and a multiple component feature around 506 cm^{-1} which is due to the Si–Si bonding in the $Si_{0.8}Ge_{0.2}$ pseudosubstrate. The shift of the Raman peak towards lower wave numbers is typical for a film under tensile stress, and the position of the strained Si–Si bonds peak is confirmed by Welser *et al.* in Ref. 17. A downward shift of 7 cm^{-1} corresponds to a tensile strain of ~1%, which is equivalent to a stress value of 1.7 GPa.[24] The shift to 506

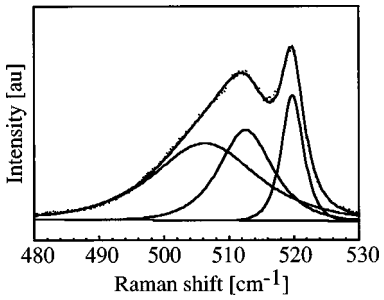

FIG. 2. Raman spectrum showing the Si–Si vibration of the strained silicon substrate. The substrate Si–Si vibration is at 520 cm^{-1}, the Si–Si vibration of the tensile-strained Si layer is at 513 cm^{-1}, and a multiple component centered around 506 cm^{-1} is attributed to the Si–Si bonding in the $Si_{0.8}Ge_{0.2}$ pseudosubstrate.

cm^{-1} is accompanied by an increase of the full width at half maximum of the peak. This increase has been observed by several authors such as Bean *et al.* in Ref. 25 and Cerdeira *et al.* in Ref. 26 and may have several origins. Possibilities include: alloying with Ge, increased defect density, and strain variations (due to defects or partial relaxation). The position of the alloyed Si contribution to the Raman spectrum is consistent with a 20% Ge concentration. The complete relaxation of the $Si_{1-x}Ge_x$ layer has been confirmed by x-ray diffraction measurements.

A 100 Å thick Ni film has been deposited on 400 Å thick strained Si layers. After *in situ* annealing, R_s has been measured by the four-point probe method. Figure 3 displays the resistivity versus the annealing temperature. The sheet resistivity is given by the multiplication of R_s, weighted by a geometry factor,[27] with the thickness of the layer. Calculated on the basis of a 100 Å thick Ni layer, the thickness of the NiSi layer is 300 Å and the thickness of the $NiSi_2$ is 360 Å which means that, respectively, ~180 Å and ~360 Å of Si are consumed by the reactions. Figure 3 shows that the sheet resistivity remains stable at 30–35 $\mu\Omega$ cm up to an annealing temperature of 700 °C and increases significantly to a value of 100 $\mu\Omega$ cm after annealing at 900 °C. Also shown in Fig. 3 is a plot of the sheet resistivity of Ni silicides formed from reaction of Ni deposited onto bulk Si(100). In that case, the resistivity increase is initiated after an annealing at 600 °C and reaches values of 130 $\mu\Omega$ cm at 850 °C. Thus the resistivity of the strained structure displays a delay of 100 °C in the resistivity stability. This means either a delayed phase transition from NiSi to $NiSi_2$ or a delayed morphology modification of the NiSi layer.

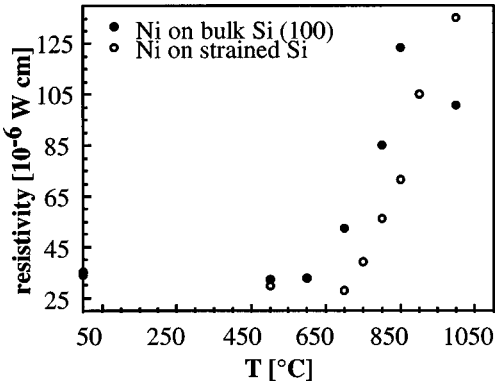

FIG. 3. Sheet resistivity vs annealing temperature for Ni deposited on bulk Si(100) and strained Si.

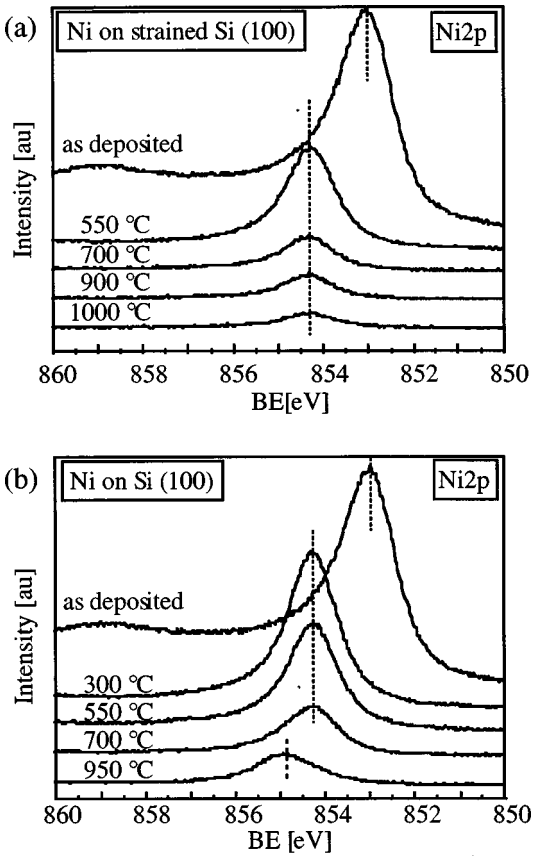

FIG. 4. XPS spectra showing the annealing dependence of the Ni2p peak for (a) Ni on strained Si and (b) Ni on bulk Si(100).

XPS analysis has been performed in order to determine the temperature at which the silicide phase transition occurs under our experiment conditions. Figures 4(a) and 4(b), respectively, show the Ni2p peak around 853 eV binding energy (BE) for Ni on bulk Si(100) and Ni on strained Si at temperatures ranging from room temperature (RT) to 1000 °C. The shift of 1.25 eV towards higher BE after an annealing at 300 °C corresponds to the formation of NiSi.[8] In the case of the formation of Ni silicide on strained Si, the Ni2p peak does not suffer any other energy shift meaning that no other phase transition occurs after annealing up to 900 °C. A further shift to higher BE is, however, observed for Ni silicide grown on bulk Si(100). After an annealing at 950 °C, the Ni2p peak is observed at 855 eV BE indicating a phase transition to $NiSi_2$. We note that the high temperature of the NiSi–$NiSi_2$ phase transitions indicates that it cannot be responsible for the measured resistivity instabilities (occurring between 600 and 700 °C).

Morphology instabilities however are shown by SEM measurements. SEM images of the NiSi film before and after the increase in sheet resistivity are presented in Figs. 5(a) to 5(d). After an annealing at 700 °C, the NiSi grown on strained Si forms a uniform film with no islanding [Fig. 5(a)]. In contrast, for the NiSi grown on bulk Si(100), island-

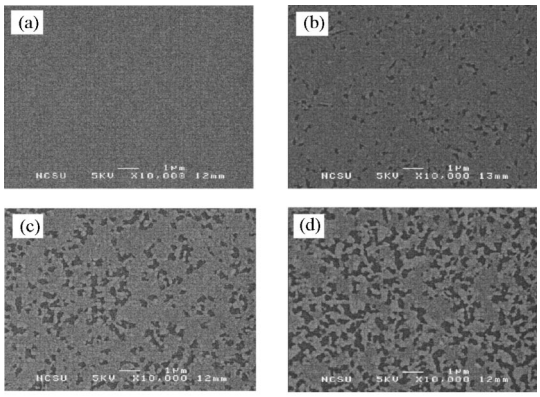

FIG. 5. SEM images of (a) Ni on strained Si after annealing at 700 °C, (b) Ni on bulk Si(100) after annealing at 600 °C, (c) Ni on strained Si after annealing at 850 °C, and (d) Ni on bulk Si(100) after annealing at 850 °C. In the image the NiSi is gray and the Si is the darker region.

ing is already observed at 600 °C [Fig. 5 (b)]. After annealing at 850 °C, both NiSi films show islanding with, however, significantly larger islands for the case of NiSi on strained Si [Figs. 5(c) and 5(d)].

The delayed morphology changes are observed more readily by *in situ* PEEM measurements where *in situ* annealing and real-time imaging were performed. Figure 6 shows 50 μm diam fields of view of NiSi on bulk Si(100) and strained Si. In our case, contrast is rather produced by topography variations than by variations of the photothreshold in the investigated sample region. The islanding of NiSi initiates at 625 °C on bulk Si(100) [Fig. 6(b)] and at 700 °C [Fig. 6(a)] on strained Si. We again notice larger islands on strained Si. Then, at an annealing temperature of 750 °C, the density of islands is observed to increase on bulk Si(100), with a decrease in the islands size [Fig. 6(d)]. However, on strained Si the NiSi islands density is observed to increase only after annealing at 850 °C [Fig. 6(c)].

We conclude that the delayed islanding of the NiSi film on strained Si is directly related to the delay in the sheet resisitivity increase (Fig. 3). It is well established that the charge carriers mobility is modified by defects and/or discontinuities in the conductive film.[11]

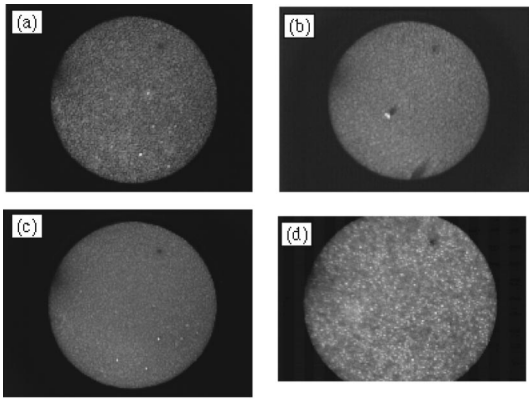

FIG. 6. PEEM of (a) Ni on strained Si after annealing at 700 °C, (b) Ni on bulk Si(100) after annealing at 625 °C, (c) Ni on strained Si after annealing at 850 °C, and (d) Ni on bulk Si(100) after annealing at 850 °C. All images were excited with a 100 W Hg lamp, and the data are displayed with a 50 μm diam field of view.

TABLE I. Lattice parameters at RT and 500 °C.

Temperature	Si	Strained Si	NiSi
RT	5.43 Å	5.47Å	5.23Å
500 °C	5.46 Å	5.5 Å	>5.5 Å[a]

[a]Ref. 31.

Islanding depends on the surface energies of the substrate and the overlayer. If the surface free energy of the overlayer is larger than the surface free energy of the substrate, the overlayer forms three-dimensional clusters (Volmer–Weber growth).[28] If the sum of the surface energy of the overlayer and the interface energy is less than the surface energy of the substrate, then the capillarity model predicts uniform film growth (or layer-by-layer growth).[29] Since the surface free energy of NiSi is 2450 $mJ\,m^{-2}$ (Ni) and that of Si is 1250 $mJ\,m^{-2}$ [Si(100)], we expect that the NiSi will form islands on Si. The lattice mismatch plays an important role. As the strain energy is a part of the surface energy,[30] the role of the interface stress is not negligible in the islanding process either.

We note that the surface morphology changes appear after annealing of the sample at 600 °C. This is higher than the transition temperature to NiSi which occurs at about 500 °C and lower than the temperature for the transition to $NiSi_2$. It is interesting to explore the role of strain in this transition. At room temperature, the lattice parameter is 5.43 Å for Si, 5.47 Å for epitaxial Si on $Si_{0.8}Ge_{0.2}$, and 5.23 Å for NiSi (Table I). Initially, at room temperature, the NiSi film is under tensile strain. As the coefficient of thermal expansion of NiSi is much larger than Si,[31] at 500 °C, a NiSi film on Si would be in compression. Since the lattice parameter of strained Si on $Si_{0.8}Ge_{0.2}$ is 0.7% larger than that of bulk Si(100), the interface stress between the NiSi film and the substrate is lower in the case of a strained Si substrate. If strain is an important aspect in driving the islanding process then a higher annealing temperature would be required to initiate islanding for NiSi on strained Si substrates. We propose that this effect contributes to the improved thermal stability of the NiSi film.

IV. CONCLUSIONS

By depositing Si onto a relaxed $Si_{0.8}Ge_{0.2}$ pseudosubstrate, we have produced a strained Si(100) substrate. A NiSi film grown on such a substrate has proven to be thermally more stable than NiSi grown on bulk Si(100). Sheet resistivity of the Ni silicide has been found to increase after annealing at 600 °C when deposited on bulk Si(100) and after annealing at 700 °C when deposited on strained Si. The phase transition to $NiSi_2$ appears after an annealing at 900 °C and is apparently not responsible for the measured resistivity increase. We suggest that islanding of the NiSi film produces the resistivity variations. SEM and PEEM investigations display islanding of the NiSi film with the islanding process occurring at an annealing temperature 100 °C higher on the strained Si substrate. The stress at the interface produced by

thermal expansion of the NiSi during the annealing process is lower in the case of the strained Si substrate because of the larger lattice parameter. We propose that this effect contributes to the observation of a higher annealing temperature to initiate the islanding of NiSi on strained Si. Therefore, NiSi on strained Si exhibits improved NiSi thermal stability over NiSi on bulk Si.

ACKNOWLEDGMENTS

This work was supported in part by the US National Science Foundation and by the Swiss National Foundation. The authors would like to thank D. Alexson for the Raman measurements and Dr. D. Bachelor for the SEM images.

[1] R. T. Tung, A. F. J. Levi, and J. M. Gibson, J. Vac. Sci. Technol. B **4**, 1435 (1986).
[2] D. X. Xu, S. R. Das, C. J. Peters, and L. E. Erickson, Thin Solid Films (submitted).
[3] F. M. d'Heurle, J. Vac. Sci. Technol. A **7**, 1467 (1989).
[4] F. M. d'Heurle, C. S. Petersson, J. E. E. Baglin, S. J. LaPlaca, and C. Y. Wong, J. Appl. Phys. **55**, 4208 (1984).
[5] D. Hesse, P. Werner, J. Heydenreich, and R. Mattheis, IEEE Electron Device Lett., 277 (1993).
[6] E. G. Colgan, J. P. Gambino, and B. Cunningham, Mater. Chem. Phys. **46**, 209 (1996).
[7] P. J. Grunthaner, F. J. Grunthaner, and J. W. Mayer, J. Vac. Sci. Technol. **17**, 924 (1980).
[8] N. W. Cheung, P. J. Grunthaner, F. J. Grunthaner, J. W. Mayer, and B. M. Ullrich, J. Vac. Sci. Technol. **18**, 917 (1981).
[9] T. Asakawa, K. Tanaka, and I. Toyoshima, J. Phys. Chem. **95**, 4783 (1991).
[10] K. N. Tu, W. K. Chu, and J. W. Mayer, Thin Solid Films **25**, 403 (1975).
[11] N. Artunc and Z. Z. Ozturk, J. Phys.: Condens. Matter **5**, 559 (1993).
[12] S. Ino, T. Yamanaka, and S. Ito, Surf. Sci. **283**, 319 (1993).
[13] J. T. Mayer and E. Garfunkel, *Nanostructured Materials* (Elsevier Science, New York, 1994), Vol. 4, No. 3, p. 275.
[14] Y. Z. Feng and Z. Q. Wu, J. Mater. Sci. Lett. **15**, 2000 (1996).
[15] H. von Kaenel, J. Henz, M. Ospelt, J. Hugi, E. Mueller, N. Onda, and A. Gruhle, Thin Solid Films **184**, 295 (1990).
[16] F. Chollet, P. Warren, D. Dutartre, and E. Andre, Jpn. J. Appl. Phys., Part 1 **33**, 6437 (1994).
[17] J. Welser, J. L. Hoyt, S. Takagi and J. F. Gibbons, Tech. Dig. Int. Electron Devices Meet. **1994**, (373).
[18] J. Welser, Mater. Res. Soc. Symp. Proc. **379**, 309 (1995).
[19] J. W. Matthews and A. E. Blakeslee, J. Cryst. Growth **27**, 118 (1974).
[20] K. Ismail, F. K. LeGoues, K. L. Saenger, M. Arafa, J. O. Chu, P. M. Mooney, and B. S. Meyerson, Phys. Rev. Lett. **73**, 3447 (1994).
[21] O. Schmidt, C. Ziethen, G. H. Fecher, M. Merkel, M. Escher, D. Menke, U. Kleineberg, U. Heinzmann, and G. Schoenhense, J. Electron Spectrosc. Relat. Phenom., 1009 (1998).
[22] G. Schoenhense and C. M. Schneider, Phys. Bl. , 1213 (1997).
[23] J. Welser, J. L. Hoyt, and J. F. Gibbons, Jpn. J. Appl. Phys., Part 1 **33**, 2419 (1994).
[24] G. Abstreiter, H. Brugger, T. Wolf, H. Jorke, and H. J. Herzog, Phys. Rev. Lett. **54**, 2441 (1985).
[25] J. C. Bean, L. C. Feldman, A. T. Fiory, and S. Nakahara, J. Vac. Sci. Technol. A **2**, 436 (1984).
[26] F. Cerdeira, A. Pinczuk, J. C. Bean, B. Batlogg, and B. A. Wilson, Appl. Phys. Lett. **45**, 1138 (1984).
[27] S. M. Sze, *Physics of Semiconductor Devices*, 2nd ed. (Wiley, New York, 1981).
[28] M. Volmer and A. Weber, Z. Phys. Chem. **119**, 277 (1926).
[29] F. C. Frank and J. H. van der Merwe, Proc. R. Soc. London, Ser. A **198**, 205 (1949).
[30] J. A. Floro, C. V. Thompson, R. Carel, and P. Bristowe, J. Mater. Res. **9**, 2411 (1994).
[31] S. Nygren, D. Caffin, M. Oestling, and F. M. d'Heurle, Appl. Surf. Sci. **53**, 87 (1991).